Bone 127 (2019) 656–663

Contents lists available at ScienceDirect

Bone

journal homepage: www.elsevier.com/locate/bone

Full Length Article

DAla2GIP antagonizes H_2O_2-induced chondrocyte apoptosis and inflammatory factor secretion

Yuze Wang[a], Chuan Xiang[a], Xiaojuan Sun[a], Song Wu[a], Jia Lv[a], Pengcui Li[a], Xiaochun Wei[a,*], Lei Wei[a,b,**]

[a] Department of Orthopaedics, The Second Hospital of Shanxi Medical University, Taiyuan City, Shanxi Province, China
[b] Department of Orthopaedics, The Warren Alpert Medical School of Brown University/Rhode Island Hospital (RIH), Providence, RI, USA

ARTICLE INFO

Keywords:
Osteoarthritis (OA)
Chondrocyte apoptosis
Inflammatory factor
PI3K/Akt/NF-κB pathway
Non-invasive calcium detection

ABSTRACT

Objective: To investigate the protective effects of DAla2GIP against the apoptosis and inflammatory factor secretion in H_2O_2-induced chondrocyte, and explore the possible mechanisms of DAla2GIP underlying its protection.

Methods: The chondrocytes were divided into the following four groups: Control, 300 μM H_2O_2, 100 pM DAla2GIP and 300 μM H_2O_2 + 100 pM DAla2GIP. The apoptosis of chondrocyte was measured by using mitochondrial membrane potential assay kit (JC-1) and TUNEL assay, the inflammatory factor secretion were assessed by ELISA assay, and the cellular and molecular mechanisms of DAla2GIP protection were investigated by using Real time-PCR, flow cytometry, Non- invasive calcium detection and western blotting techniques.

Results: (1) DAPla2GIP prevents apoptosis of chondrocyte induced by H_2O_2. (2) DAla2GIP alleviated the inflammation of chondrocyte induced by H_2O_2. (3) DAla2GIP prevents chondrocyte apoptosis by inhibiting calcium influx of chondrocyte and regulating expression of Bcl-2 and Caspase-3induced by H_2O_2. (4) DAla2GIP inhibited the H_2O_2 mediated inflammation by up- regulating the expressions of Sox9 and Col2a1 and inhibiting PI3K/Akt/NF-κB pathway.

Conclusion: Our experimental results revealed that DAla2GIP prevents chondrocyte apoptosis by inhibiting calcium influx of chondrocyte and induced regulating expression of Bcl-2 and Casp ase-3by H_2O_2. Further, molecular biology experiments confirmed that DAla2GIP inhibited the H_2O_2 mediated inflammation vis up-regulating the expressions of Sox9 and Col2a1 and inhibiting PI3K/Akt/NF-κB pathway. The results demonstrate that DAla2GIP has protective properties in H_2O_2-induced chondrocyte injury, this finding shows that novel GIP analogues have the potential as a novel therapeutic for osteoarthritis patients.

1. Introduction

Osteoarthritis (OA) is a progressive and degenerative joint disease, with a strong impact on individual and population health. OA is a clinically heterogeneous disease presenting with different clinical phenotypes and local risk factors [1]. Clinical features of OA mainly include gradual degradation of articular cartilage, synovial inflammation and pain, resulting in significant disability. Studies have shown that chondrocytes apoptosis and degradation of the extracellular matrix (ECM) are involved in pathogenesis of OA [2,3]. Chondrocytes are the only residing cell type in cartilage and have low mitotic activity, poor intrinsic self-renewal, and inefficient healing capacity [4]. And abnormal catabolism and differentiation of chondrocytes leads to degradation of the ECM [5]. The apoptosis of chondrocytes as well as the dysregulation of ECM homeostasis have been widely considered as the main factors that cause the dysfunctions of articular cartilage. Chondrocyte apoptosis would be a valid target to modulate cartilage degeneration, because the loss of chondrocyte vitality is a significant hallmark of human OA.

Glucose-dependent insulinotropic peptide (GIP), also known as gastric inhibitory polypeptide, is secreted by intestinal enteroendocrine K cells in a nutrient-dependent manner [6]. GIP receptors are widely expressed throughout the intestine including the gut, pancreas, adrenal cortex, and adipose tissue, and in addition it is present in vascular tissue, brain, and bone [7,8]. GIP has been reported to exert an anti-apoptotic and stimulating effect on osteoblasts in vitro [9–11]. In

* Correspondence to: X. Wei, Department of Orthopaedics, The Second Hospital of Shanxi Medical University, 382 Wuyi road, Taiyuan City, Shanxi Province, China.
** Correspondence to: L. Wei, Department of Orthopaedics Brown Medical School/RIH, Coro West/402H, 1 Hoppin Street, Providence, RI 02903, USA.
E-mail addresses: sdeygksys@163.com (X. Wei), Lei_Wei@brown.edu (L. Wei).

https://doi.org/10.1016/j.bone.2019.05.026
Received 6 December 2018; Received in revised form 16 May 2019; Accepted 19 May 2019
Available online 05 July 2019

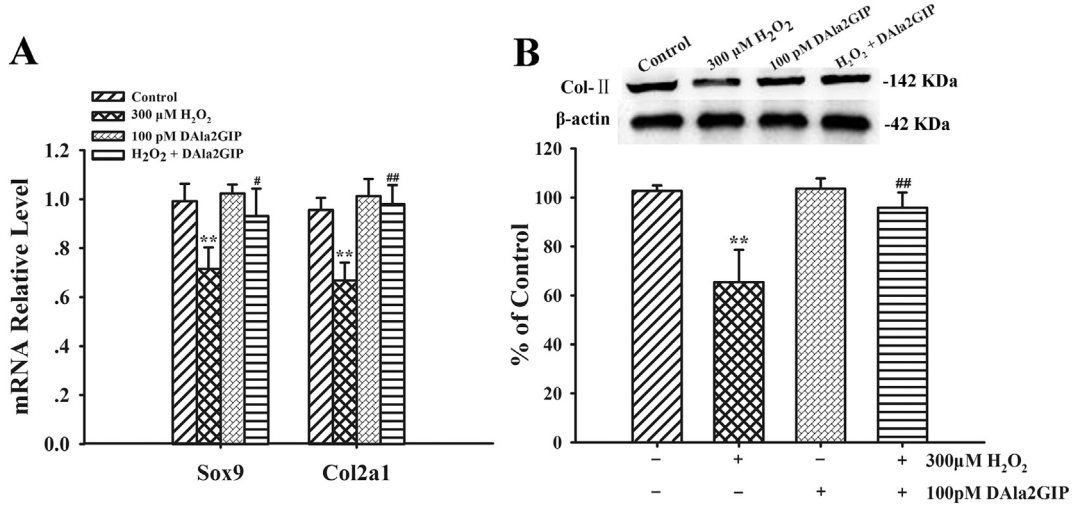

Fig. 1. The regulation effects of H_2O_2 or DAla2GIP on the expression levels of Sox9 and Col2a1 in chondrocytes. A: Histograms showing the differential regulation of H_2O_2 or DAla2GIP on the Sox9 and Col2a1 mRNA. **P < 0.01 vs control group, #P < 0.05 and ##P < 0.01 vs H_2O_2 group. B: The protein band with western-blotting. Loading control was settled with β-actin. And Statistical analysis bar chart to show the protein level of Col-II in different groups. **P < 0.01 vs control, ##P < 0.01 vs H_2O_2 group.

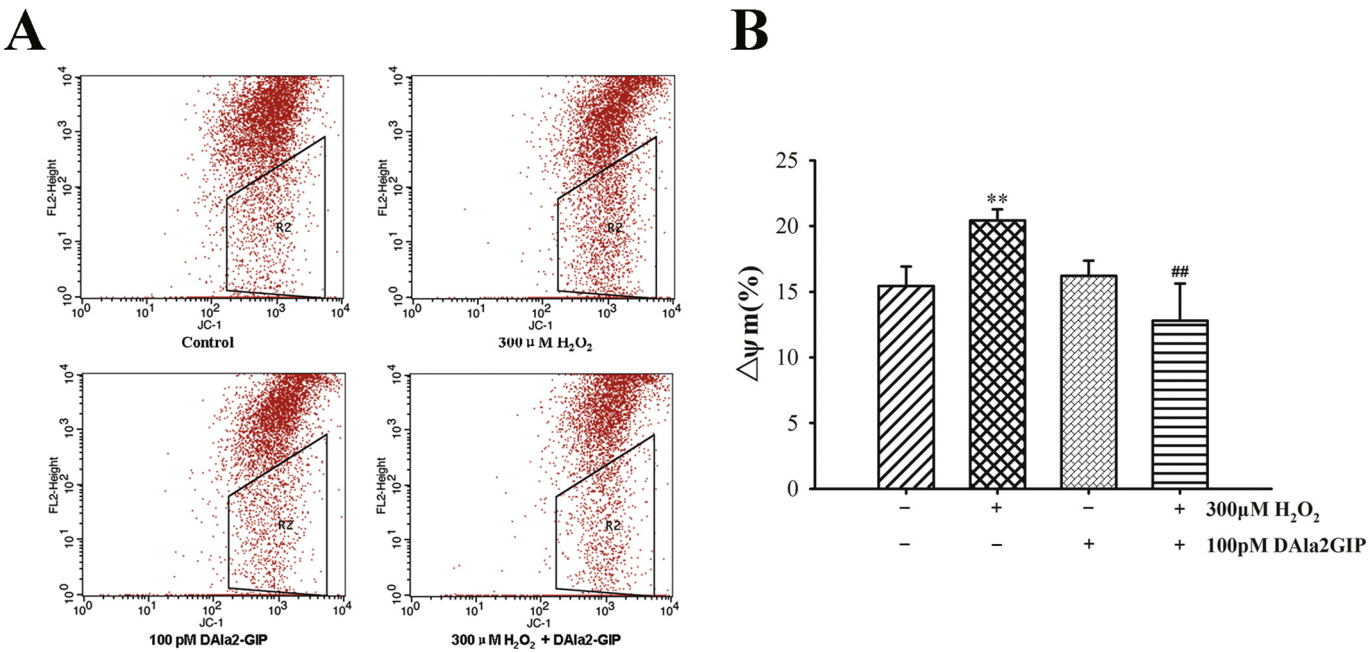

Fig. 2. Effects of DAla2GIP to mitochondrial membrane potential induced by H_2O_2. A: Representative cell distribution plots in four groups. Cells were measured by flow cytometry. Skew box outside: from JC-1 aggregates in normal cells with high polarized mitochondrial membrane potential. Skew box inside: from JC-1 monomers in apoptotic cells with depolarized mitochondrial membrane potential. B: Histograms showing statistical analysis to compare the membrane potential among different groups. ** P < 0.01 vs control; ## P < 0.01 vs H_2O_2 group.

animal models, increased numbers of osteoblasts and increased serum concentrations of osteocalcin, a bone formation marker, were observed in response to GIP over expression [12]. But the rapid degradation of GIP in plasma by dipeptidyl peptidase-IV (DPP-IV) precludes to its use as a therapeutic approach [13]. DAla2GIP is the analogue of GIP, which could enhance the resistance to degradation by DPP-IV and prolong the half-life to 5–6 h in the body. However, this novel GIP analogue has not been tested whether it has protective properties in cultured chondrocytes.

Therefore, the aims of the present study were to investigate whether DAla2GIP directly inhibit the apoptosis and the secretion of inflammatory factors of chondrocytes, and to decipher what molecular pathways were necessary for such effects.

2. Material and methods

2.1. Experimental reagents

DAla2GIP was purchased from Qiangyao Biotech Inc. (Su Zhou/Shang Hai, China). Primary antibodies (Anti-PI3K p85; ab189403; Anti-AKT1-phosph S473, ab66138, Abcam; Anti-NF-κB p65 (Ser468), 3039, Cell Signaling Technology; USA, Anti-Collagen II antibody ab34712, Abcame, UK), secondary antibodies (Biotin-Goat anti-Mouse IgG, BST10G22C01, Biotin-Goat anti-Rabbit IgG, BST10G22C03, Boster Biological Technology, China) as well as fluorescent labelled primary antibodies (FITC Rabbit Anti-Active Caspase-3, 559,341; FITC Hamster Anti-Mouse Bcl-2 Set: 554221, BD Pharmingen™) were used for western

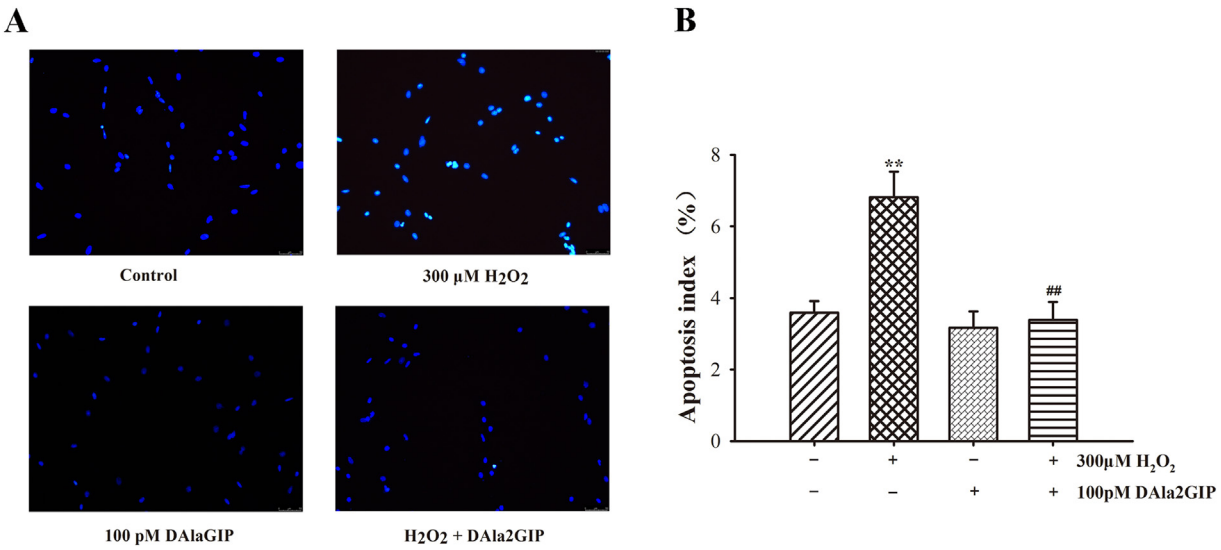

Fig. 3. DAla2GIP treatment reduced chondrocytes apoptosis. A: Photographs showing TUNEL staining of chondrocytes treated with H_2O_2 or DAla2GIP. Apoptotic chondrocytes were stained with fluorescein-dUTP (green) and cell nuclei were stained with DAPI (blue), the photographs were 20 × 10 fluorescence microscope image. B: Histograms showing statistical analysis of TUNEL staining among different groups. **P < 0.01 vs control; ## P < 0.01 vs H_2O_2 group. (For interpretation of the references to color in this figure legend, the reader is referred to the web version of this article.)

Table 1
Secretion Level of TNF-α and MMP13 in Different Groups (mean ± SD, n = 6).

Group	TNF-α (ng/ml)	MMP-13 (ng/ml)
Control	9.0077 ± 2.0282	11.3107 ± 1.8697
300 μM H_2O_2	18.9028 ± 2.9716**	20.2224 ± 2.4453**
100 pM DAla2GIP	9.5787 ± 2.2672	9.5557 ± 1.5146
H_2O_2 ± DAla2GIP	10.5155 ± 2.0084##	10.3192 ± 1.0290##
F value	F = 23.391	F = 46.136

** P < 0.01 vs Control.
P < 0.01 vs 300 μM H_2O_2.

blot assay and flow cytometry respectively. ELISA kit for Tumor Necrosis Factor-α (TNF-α) (SEA133Mu) and ELISA kit for Matric Metalloproteinase 13 (MMP13) (SEA099Mu) were purchased from CLOUD-CLONE CORP. (CCC, USA). For Real-time PCR, Trizol reagent was purchased from Carlsbad (Carlsbad, Carlsbad, USA), GoScript™ Reverse Transcription Mix (A2791) and GoTaq® qPCR Master Mix (A6001) were purchased from Promega (Promega, USA). All reagent used for cell culture was purchased from Gibco Inc. US. CCK- 8 kit used for cell validity assay was obtained from Dojindo Inc. JC-1 kit, which used for mitochondrial membrane potential detecting was obtained from Beyotime Inc., Shanghai, China. In the experiment, Dala2GIP was dissolved into saline with concentration of 10 nM and stored in −20 °C.

2.2. Chondrocyte culture

7-day-old mouse was sacrificed after anesthesia with 1.0 ml ether and disinfected with 75% alcohol for 15 min. Thorax was separated and transferred into sterile PBS. The cartilage tissue attached on the thorax was carefully extracted with scissor and washed with PBS. The cartilage tissue was digested with 0.25% trypsinase and chondrocytes were inoculated into dish. Chondrocytes were subcultured when the cells fused to 80–90%, and the third generation chondrocytes were used for experiments. The cultured chondrocytes were divided in the following four groups according to different drug treatments: (1) normal control (Saline 10 μl); (2) 300 μM H_2O_2 group; (3) 100 pM DAla2GIP treatment alone; (4) 300 μM H_2O_2 + 100 pM DAla2GIP treatment. The sample size of all groups was 6.

2.3. Real time polymerase chain reaction (PCR)

Total RNA was isolated from cultured chondrocytes using Trizol reagent and was reverse-transcribed with the GoScript™ Reverse Transcription Mix. Real-time quantitative PCR amplification was performed using the GoTaq® qPCR Master Mix (A6001). mRNA levels were normalized to GAPDH and calculation of mRNA values was performed as previously described [14]. The cycle threshold (Ct) values for GAPDH and that of samples were measured and calculated using computer software (IQ50, Bio-Rad, USA). Expression levels were calculated as $x = 2^{-\triangle\triangle Ct}$, in which △ △ Ct = △ E- △ C, and △ E = Ctexp-CtGAPDH; △C = Ctctl-CtG. The sequences of the primers were as follows: Sox9 forward primer 5′-TCCAAGCGCATTACCCA CTT-3′ and reverse primer 5′-GTTGATTTCGCTGCT CCATTTA-3′, Col2a1 forward primer 5′-GGCAATAGCAGGTTCACGTACA-3′ and reverse primer 5′-CGATAACAGTCTTGCCCC ACTT-3′, GAPDH forward primer 5′-GGTGAAGGTCGGAGTGAACG-3′ and reverse primer 5′-AGT TAAAAGCAGCCCTGGTGA-3′.

2.4. Itochondrial membrane potential detection

The 3rd chondrocytes were seed in 6-well plate and incubated for 72 h. Drug treatment lasted for 24 h. The chondrocytes were washed with D-Hanks solution and then mixed with 1 mL JC-1 working fluid. The cells were incubated at 30 °C for 30 min. After incubation, the supernatant was removed and the chondrocytes were washed twice with JC-1 staining buffer. Subsequently, 0.25% trypsinase digested cells to obtain cell suspension and mitochondrial membrane potential was detected with flow cytometry (BD inc. FACS Calibur).

2.5. TUNEL assay

The 3rd chondrocytes were seeded in 6-well plates pre-loaded with coverslips, after treatment with the drugs for 48 h, the coverslips were removed and naturally dried, and fixed in 4% paraformaldehyde for 30 min at room temperature. After fixation, cells were washed with PBS for three times, cells were washed with PBS with 0.3% TritonX-100 for 5 min. TUNEL staining reagent (C1088, Beyotime Inc., Shanghai, China.) was added on the coverslip and incubate for 60 min at 37 °C in the dark. After incubation, cells were washed with PBS for three times and nucleis were stained with DAPI for 10 min. Slice was prepared with

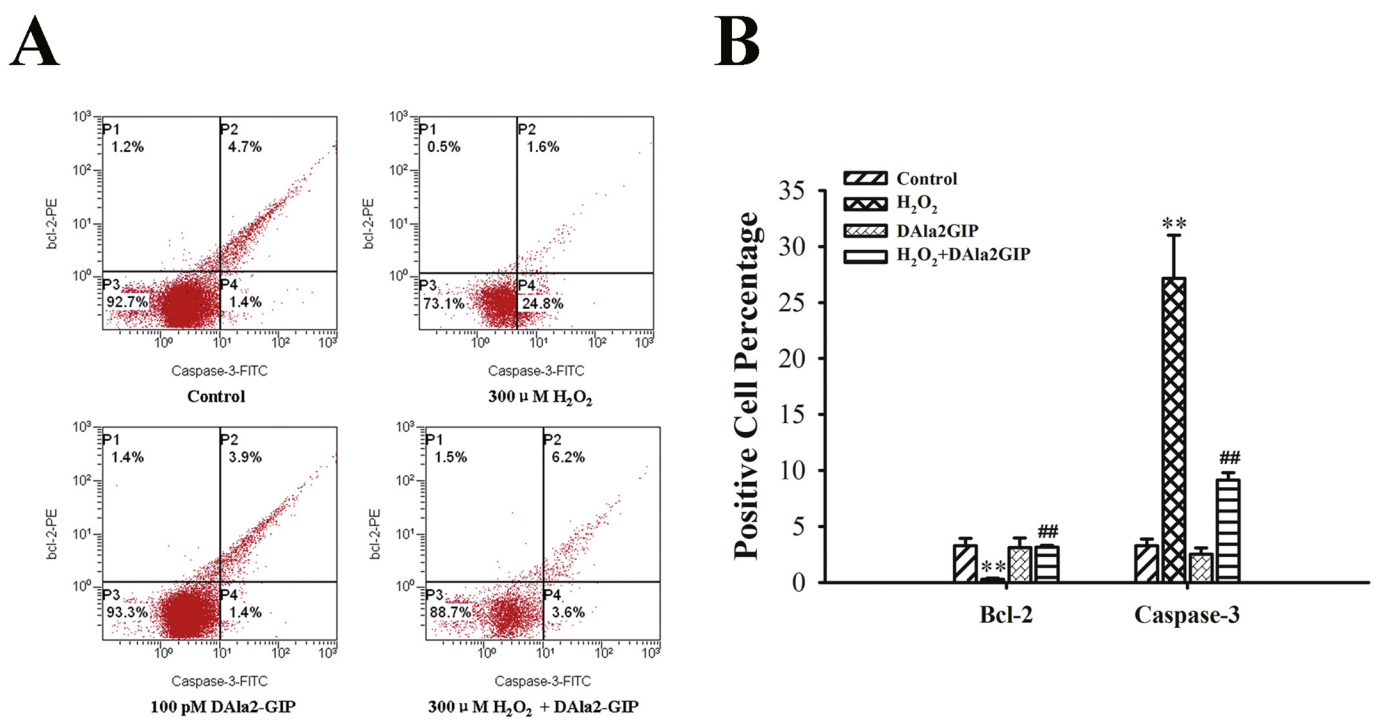

Fig. 4. Flow cytometry to show the positive chondrocyte ratio with Bcl-2 and/or Caspase-3. A: Spot chart of the flow cytometry to show the positive ratio of Bcl-2 and Caspase −3. In each plot, the lower left quadrant (P3) represents viable cells, and the lower right quadrant (P4) represents early apoptotic cells. The quadrant of P1 + P2 represents positive chondrocyte ratio with Bcl-2, and the quadrant of P1 + P2 represents positive chondrocyte ratio with Caspase-3. B: Bar chart to show the statistical analysis among different groups. **P < 0.01 vs control; ##P < 0.01 vs H_2O_2 group.

mountain medium after coverslip was washed with PBS. Cell apoptosis was detected by fluorescence microscopy.

2.6. LISA assay

Cultured medium of each group was collected for ELISA assay. ELISA detection for TNF-α and MMP-13 was performed following the product introduction. Briefly, 5 concentrations of standard were added with 3 repeat wells (50 μl per well). 50 μl dilute buffer was used for as blank control. 50 μl sample was added (3 repeats per sample) into each well. Detecting buffer A (50 μl) was added into each well and shaking for 1 h at 37 °C. Then remove the supernatant in the well and wash for 3 times and added detecting buffer B (100 μl) per well and shaking for 30 min at 37 °C. Remove detecting buffer B and wash the wells for 5 times, and add TMB substance 90 μl per well and incubate at dark for 20 min under 37 °C. The OD value was detected with plate reader at 450 nm after added the stop solution 50 μl per well.

2.7. Low cytometry

Chondrocytes were inoculated in 6-well plates and treated with drugs for 48 h. Briefly, cells were washed twice with D-Hanks solution and digested with 0.25% trypsin, cell suspension was obtained and centrifuged for 5 min at 1000 r/min. Cells were collected and added to Binding Buffer to make cell suspension with a density of 1×10^7 cells/ml. 5 μl primary antibodies (FITC rabbit active Caspase-3, FITC hamster Bcl-2) with 5 μl PI staining buffer was added into cell suspension. Cell was labelled by incubation for 20 min in the dark at room temperature. Flow cytometry was then performed to detect the positive cell population.

2.8. Non-invasive micro-test calcium detection

Detection of cellular calcium was performed in 25 mm dish. Briefly, glass microsensor (dimeter of the tip is 1–2 μm) was filled with 100 mmol/L CaCl2 (with length of 1 cm) and pushed into the end. Then Ca^{2+} ion exchange buffer LIX (XY-SJ-Ca, Younger USA, Amherst, MA, US) was sucked into the end of microsensor (with length of 40–50 μm). The Ag/AgCl electrode was inserted into the detector within the detection buffer. Then the microsensor was connected to voltage detector. Ag/AgCl electrode (DRIREF-2; World Precision Instruments) is settled as reference, which was attached in the perfusion buffer and connected to ground. Different concentration of $Ca2^+$ (3 and 0.3 mmol/L) dissolved in the aCSF (NaCl 10 mmol/L, KCl 3 mmol/L, NaH2PO4 1.25 mmol/L, NaHCO3 25 mmol/L, D-glucose 10 mmol/L, MgCl2 1 mmol/L, CaCl2 2.5 mmol/L, pH 7.3–7.4) was used as correction buffer. The cellular detecting was started when logarithm of voltage/concentration reached 22 mV/decade. The electrode was attached into the aCSF with the distance to cell around 20 μm, which was used for assess near and far position. The movement frequency of electrode was settled as 0.3 Hz and the difference of voltage (dv) between two positions could be recorded. Then the difference of Ca^{2+} concentration (dc) could be obtained from the logarithm of voltage/concentration. Ca^{2+} diffusion J could be calculated with the algorithm ($J = -D \times dc/dx$ D: ion/molecular specific diffusion constant), which reflects the flow of Ca^{2+} at certain area during certain time (pmol·cm^{-2}·s^{-1}). Positive J value means the extracellular flow of Ca^{2+}, while the negative value stand for the intracellular flow.

2.9. Western blot assay

Chondrocytes protein lysate was prepared with RIPA buffer. Protein concentration was measured using bicinchoninic acid (BCA) protein assay kit. A total of 50 μg of protein from each sample was used. Sample proteins in all groups were separated on 12% SDS-PAGE. Proteins was transferred into PVDF membrane and nonspecific binding was blocked with 5% BSA in Tris-buffered saline containing 0.05% Tween-20 (TBST) for 2 h. Membrane was then incubated with primary antibodies (anti-PI3K p-85 1:3000; anti-Akt-pS473 1:600; anti-NF- κB-p65 1:1000; anti-Collagen II antibody 1:6000; β-actin 1:3000) overnight at 4 °C. After

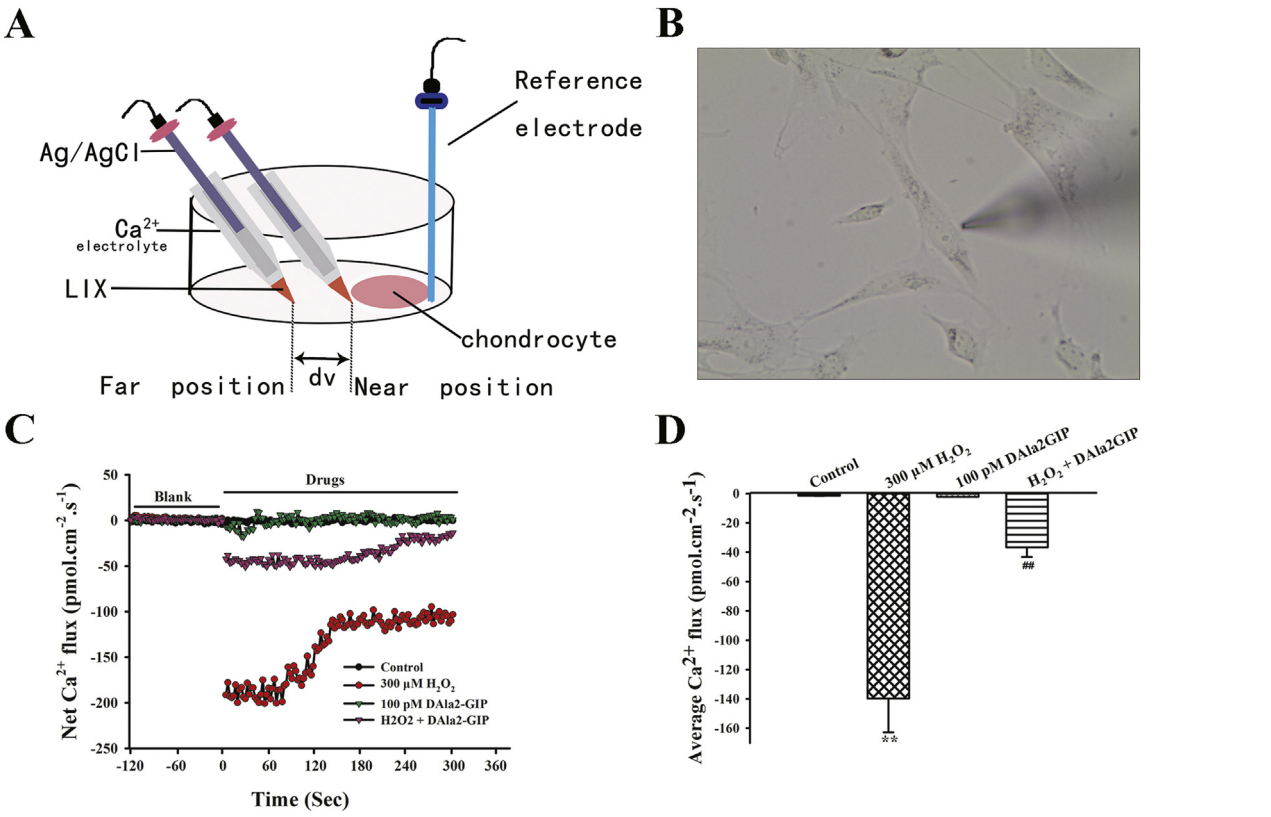

Fig. 5. Measurement of $Ca2^{+}$ fux of chondrocytes by using NMT. A: A diagram showing the principle of NMT ion flux measurements. Ca^{2+} sensitive microelectrode (silver gray) flled with Ca^{2+} LIX and 100 mmol/L Ca^{2+} electrolyte oscillated between far and near positions, with a fixed distance (30 μm). The reference electrode (blue) was in the same dish. B: Screen-printed pictures showing that the microelectrode located at the margin of the chondrocytes. C and D: After acute application of H_2O_2 or DAla2GIP, the transmembrane Ca^{2+} influx in the chondrocytes, B, Plots showing the time courses of chondrocyte net Ca^{2+} flux in the chondrocytes. A basic Ca^{2+} flux was first recorded for 120 s (−120 to 0 s) before drug application. Negative deflection of curves indicates Ca^{2+} influx. C, Histograms showing the statistical analyses of average Ca^{2+} influx during 300 s following drugs application. Columns and error bars represent means ± SD. **: $P < 0.01$ vs control, ##: $P < 0.01$ vs H_2O_2 group. (For interpretation of the references to color in this figure legend, the reader is referred to the web version of this article.)

Table 2
Gray Value of the Phosphorylated Proteins in Different Groups (mean ± SD, n = 6).

Group	PI3K (p85)	p-AKT1 (S473)	NF-κBp65 (Ser468)
Control	100.0000 ± 22.2973	100.0000 ± 12.1636	100.0000 ± 35.8122
300 μM H_2O_2	149.6431 ± 42.0818**	152.5396 ± 27.6287**	192.7055 ± 66.2714**
100 pM DAla2GIP	99.4858 ± 18.7873	107.8813 ± 18.9316	104.5209 ± 36.3023
H_2O_2 ± DAla2GIP	112.6689 ± 27.8656#	115.5871 ± 18.0251##	113.1659 ± 41.0497##
F value	3.933	8.133	5.293

** $P < 0.01$ vs Control.
# $P < 0.05$.
$P < 0.01$ vs 300 μM H_2O_2.

incubation, membrane was washed with TBST for 3 times (5 min per time) and incubated with secondary antibody (Goat-anti-rabbit-HRP, 1:3000) for 2 h at 4 °C. Then wash the membrane with TBST for 3 times and protein bands were obtained with ECL reagent in the imager. Alpha view SA software was used for analyze the density of the bands. β-actin was utilized as an internal control for sample loading, and each blot was normalized to its corresponding β-actin value.

2.10. Statistic

All values are expressed as means ± SD, and all other data were analyzed by One-way ANOVA (Tamhane's T2 test was performed with heterogeneity of variance). Statistical significance was defined as $P < 0.05$, and all statistical analyses were performed using the statistical software packages SPSS 18.0.

3. Results

3.1. The effect DAla2GIP treatment on the expression of chondrogenic markers

To investigate the effect of DAla2GIP treatment on the expression of chondrogenic markers, we examined the expression level of chondrocytes Sox9 and Col2a1. As shown in Fig. 1A, compared with control group, the level of Sox9 (0.71 ± 0.09) and Col2a1 (0.67 ± 0.07) mRNA significantly decreased ($P < 0.01$) in H_2O_2 alone group, DAla2GIP pretreatment effectively reversed H_2O_2-induced changes in the gene expression, the mRNA expression of Sox9 (0.93 ± 0.11, $P < 0.05$) and Col2a1 (0.98 ± 0.08, $P < 0.01$) significantly increased compared to H_2O_2 alone group. We next examined the type II collagen (Col-II) protein levels of all groups, as shown in Fig. 1B, the protein level of Col-II (65.37% ± 13.25%) was markedly reduced in

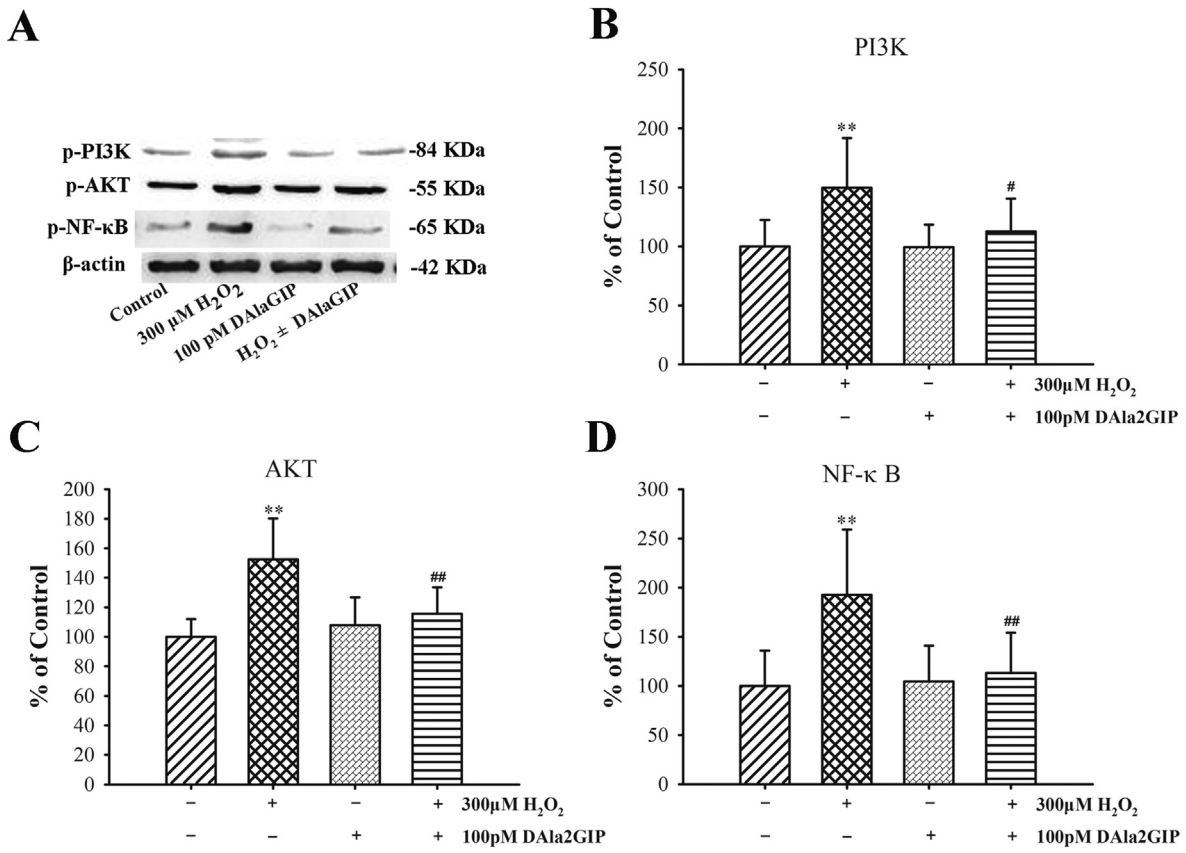

Fig. 6. The effects of DAla2GIP to protein phosphorylation in different groups. A: The phosphorylated protein band images in different groups. DAla2GIP reversed the changes of phosphorylated protein content in H_2O_2-induced disruption in the levels of protein. Loading control was settled with β-actin. B, C, D: Statistical analysis bar chart to show the relative gray values on protein level of pPI3K, pAkt and pNF-κB in different groups. **P < 0.01 vs control, #P < 0.05 vs H_2O_2 group, ##P < 0.01 vs H_2O_2 group.

H_2O_2 alone group compared to control group (102.7% ± 2.22%, P < 0.01), DAla2GIP incubation effectively counteract H_2O_2-induced disruption in the levels of Col-II, the protein level of Col-IIin H_2O_2 + DAla2GIP was 95.73% ± 6.3%, significantly higher than the value in H_2O_2 group (P < 0.01), there were no significant statistical difference (P > 0.05) of the protein level between control group and DAla2GIP alone group.

3.2. DAPla2GIP prevents apoptosis of chondrocyte induced by H_2O_2

At the early onset of apoptosis, an increasing of permeability of mitochondrial membrane presents in the cell. For detecting the effects of DAla2GIP to H_2O_2 induced apoptosis, we performed the mitochondrial membrane potential test (JC-1). As shown in Fig. 2B, compared with control group (△ Ψm, 15.4317% ± 1.4866%), 300 μM H_2O_2 treatment caused the increasing mitochondrial membrane potential depolarization cell ratio (△Ψm, 20.4150% ± 0.8536%, P < 0.01). While treatment of 100 pM DAla2GIP presented the alleviated mitochondrial membrane potential depolarization cell ratio (△ Ψm, 16.2117% ± 1.1533%, P < 0.01) in comparing with H_2O_2 model group. Additionally, administration with 100 pM DAla2GIP alone (△Ψm, 12.7867% ± 2.8340%) did not show significant different compared with control. Meanwhile, we also performed TUNEL staining to confirm the apoptotic conditions. As shown in Fig. 3A and B, 300 μM H_2O_2 treatment (6.8133 ± 0.7151) presented a remarkable higher rate of apoptosis compared with control group (3.5967 ± 0.3223, P < 0.01). Likewise, combination treatment with 100 pM DAla2GIP reduced the apoptosis (3.1717 ± 0.457, P < 0.01). While treatment of DAla2GIP alone (3.3917 ± 0.5037, P > 0.05) did not affect the apoptotic rate compared with control.

3.3. DAla2GIP alleviated the inflammation of chondrocyte induced by H_2O_2

To observe the effect of DAla2GIP to inflammatory reaction induced by H_2O_2, we detected the level of TNF-α and MMP13 in cultural medium with ELISA assay. As shown in Table 1, incubation with 300 μM H_2O_2 for 24 h induced the significant increasing of TNF-α and MMP13 compared with control group (P < 0.01). While pre-treatment with 100 pM DAla2GIP resulted in the remarkably decreased secretion of these two inflammatory factors to medium compared with 300 μM H_2O_2 group (P < 0.01). Treatment of 100 pM DAla2GIP alone showed no significant difference in comparing with control group (P > 0.05).

3.4. DAla2GIP prevents apoptosis by regulating expression of Bcl-2 and Caspase-3

To exploring the mechanism of DAla2GIP in inhibiting apoptosis, we employed flow cytometry to test positive ratio of Bcl-2 and Caspase-3 in chondrocytes. As shown with Fig. 4, compared with control (Bcl-2: 3.2833 ± 0.6395, Caspase-3: 3.2667 ± 0.6075), 300 μM H_2O_2 induced dramatic decreased ratio of Bcl-2 (0.2833 ± 0.0872, P < 0.01) and increasing of Caspase-3 (27.1667 ± 3.8388, P < 0.01). Compared with H_2O_2 group, pre-treatment of 100 pM DAla2GIP attenuated the alteration of Bcl-2 (3.1167 ± 0.8396, P < 0.01) and Caspase-3 (2.5000 ± 0.5808, P < 0.01). While single group of DAla2GIP showed no significance statistical difference compared with control group (P > 0.05).

3.5. DAla2GIP inhibits calcium influx of chondrocyte induced by H_2O_2

Influx of Ca^{2+} was widely considered as the early onset of apoptosis of chondrocytes. Therefore, we detected the Ca^{2+} dynamics with non-invasive detection. As shown in Fig. 5, the average current velocities of calcium ions within 5 min were recorded in different groups. The results show that the Ca^{2+} influx has no significant different between DAla2GIP treatment alone (-1.94 ± 0.04) and control (-1.42 ± 0.08). After 300 μM H_2O_2 treatment leaded to the obvious intracellular Ca^{2+} influx (-139.61 ± 23.27, $P < 0.01$). Combination treatment of DAla2GIP with H_2O_2 results prohibited the H_2O_2 increased Ca^{2+} influx, which reflected by significant low speed of Ca^{2+} influx speed (-26.68 ± 6.43, $P < 0.01$) compared with H_2O_2 group.

3.6. DAla2GIP inhibited the H_2O_2 mediated inflammation vis PI3K/Akt/NF-κB pathway

As shown in Table 2 and Fig. 6, incubation with 300 μM H_2O_2 induced the remarkable elevated intensity of p-PI3K, p-Akt and NF-κB (Ser468) in comparing with control ($P < 0.01$). While after pre-treated with 100 pM DAla2GIP, the intensity of protein band of p-PI3K, p-Akt and NF-κB (Ser468) underwent the remarkable decrease, which present the significance difference compared with 300 μM H_2O_2 group ($P < 0.01$). Additionally, compared with control group, treatment with DAla2GIP alone group did not affect the protein level of these three signaling factors ($P > 0.05$).

4. Discussion

OA is characterized by progressive destruction of articular cartilage, resulting in significant disability. Chondrocytes, the only cells in articular cartilage, are critical in the pathological progression of OA via apoptosis and cytokine production [15]. The survival of the chondrocytes is important for the maintenance of proper cartilage matrix, and the compromising of chondrocyte function and survival would lead to the failure of the articular cartilage [16]. Apoptosis clearly occurs in osteoarthritic cartilage, however, the relative contribution of chondrocyte apoptosisin the pathogenesis of OA is difficult to evaluate. GIP is widely expressed in multiple tissues including cartilage tissue and has wide range of physiological functions. It has been reported that GIP prevents serum deprivation-induced apoptosis in human bone marrow-derived [17]. Mabilleau et al. [18] confirmed that GIP dose- dependently reduces osteoclast differentiation and resorption. GIP directly affects collagen fibril diameter and collagen cross-linking in osteoblast cultures [10]. Aleksandra et al. found that GIP receptor deletion leads to reduced bone strength and quality [19]. All those lines of evidence suggest that GIP plays crucial roles in regulating bone growth. In the present study, our results of mitochondrial membrane potential and TUNEL shown that GIP agonist DAla2GIP effectively inhibited H_2O_2-induced mitochondrial membrane potential depolarization ($\triangle\Psi m$) and reduced chondrocytes apoptosis. These results are consistent with previous reports, Maneiro et.al [20] found that chondrocytes from OA cartilage showed a significant decrease in the mitochondrial membrane potential, which is related to mitochondrial swelling and damage of the outer mitochondrial membrane.

Mitochondria play a key role in cellular function and survival, and oxidative stress and disrupted mitochondrial respiration were reported to promote cell death and degeneration. Mitochondrial membrane potential abnormally elevated the early onset of the apoptosis [21]. Depolarization of the mitochondria leads to the release of apoptotic factors, such as cytochrome *c* (cyt c), apoptosis-inducing factor and caspase-9, from the mitochondrial inter membrane space to the cytoplasm, and then caspase-9 activates caspase-3, the most important executioner caspase, and leads to apoptosis [16]. The Bcl-2 family members control mitochondrial apoptotic signaling by modulating mitochondrial membrane permeability. Bcl- 2 exerts anti-apoptotic effect by inhibiting the release of cyt c [22]. We employed flow cytometry to test positive ratio of Bcl-2 and Caspase-3 in chondrocytes, our results found that Bcl-2 was significant decrease and caspase-3 was significant increase in 300 μM H_2O_2- induced group, and 100 pM DAla2GIP pretreatment reversed the H_2O_2-induced change in Bcl-2 and Caspase-3. Calcium ion (Ca^{2+}) is important for many cellular events, such as proliferation/growth, differentiation, development and cell death [23]. Tagliarino et al. found elevation of intracellular Ca^{2+} acts critically in trigger the early signaling of mitochondrial apoptosis and finally result in the program cell death [24]. In the present study, we confirmed that the intracellular Ca^{2+} influx in H_2O_2 group was obviously higher than that in control group, however, DAla2GIP treatment attenuated the increase of intracellular Ca^{2+} influx induced by H_2O_2. In general, our results suggested that DAla2GIP effectively inhibits H_2O_2-induced chondrocyte apoptosis. The possible mechanism is that DAla2GIP attenuates mitochondrial membrane damage by inhibiting intracellular calcium overload, which improve the inhibitory effect of Bcl-2 on mitochondrial release cyt c, caspase-3 activation and chondrocyte apoptosis were inhibited.

Chondrocytes are responsible for the maintenance of the highly specialised extracellular matrix (ECM) of articular cartilage, the transcription factor Sox9 plays an essential role in determining the fate of several cell types and is a master factor in regulation of chondrocyte development. High expression levels of Sox9 are associated with enhanced levels of Col2a1, which is an essential components for cartilage ECM [25]. The matrix metalloproteinase 13 (MMP13) is considered to perform a key role in the non-reversible destruction of the type II collagen network in OA [26]. Conventional inflammatory factors, such as IL-1β and TNF-α, can leads to cartilage ECM degradation via increased expression of MMPs [27]. In vitro study shows that TNF-α could promote chondrocytes to produce of MMPs, PGE2 and NO, all of which could inhibit the synthesis of type II collagen and aggrecan [28]. It was reported that NF-κB pathway is another important pathway which is closely related to inflammatory diseases including OA [29]. Meanwhile, stimulating of NF-κB signaling promote the self- synthesis of TNF-α [30]. In the present study, our results confirmed the level of Sox9 and Col2a1 mRNA significantly decreased in H_2O_2 alone group compared to control group, DAla2GIP pretreatment effectively reversed H_2O_2-induced changes in the gene expression, the mRNA expression of Sox9 and Col2a1 significantly increased compared to H_2O_2 alone group. At the same time, we examined the type II collagen (Col-II) protein levels of all groups, we found that the change of Col-IIprotein levels in all group was parallel to the expression of Sox9 and Col2a1. Our ELISA experiment results shown that treatment with 300 μM H_2O_2 increased the level of TNF-α and MMP-13 in medium, while 100 pM DAla2GIP attenuated such elevation. These results confirmed the protective effect of DAla2GIP on H_2O_2-induced chondrocyte inflammation response. Next, our western blotting showed that 300 μM H_2O_2 increased the activity of PI3K, Akt and NF-κB by detecting their phosphorylation level. While, treatment of 100 pM DAla2GIP reduced the phosphorylation of the above-mentioned proteins. NF-κB signaling is involved with regulating the growth, differentiation and apoptosis of the chondrocytes, and acts critically in development of OA. NF-κB is ubiquitously expressed and can be activated by multiple factors. Previous study suggests mild stimulation of NF-κB could inhibit apoptosis, while an over activation could increase the expression of many inflammatory factors and promote apoptosis [31]. Recent study also indicates that PI3K/Akt pathway is closely related with the occurrence of apoptosis and development of OA [29]. In current study, we found the increased inflammatory factors in medium was due to the over activity of the PI3K/Akt/NF-κB. Stimulated NF-κB triggers the vicious circle and enhances the inflammation response, while DAla2GIP prevents the inflammatory reaction by inhibiting such signaling.

5. Conclusions

In summary, the present study indicates that DAla2GIP prevents chondrocyte apoptosis by inhibiting mitochondrial damage caused by intracellular calcium overload, which promotes the inhibitory effect of Bcl-2 on mitochondrial release cyt c, caspase-3 activation were inhibited. Further, molecular biology experiments confirmed that DAla2GIP inhibited the H_2O_2 mediated inflammation by up-regulating the expressions of Sox9 and Col2a1 and inhibiting PI3K/Akt/NF-κB pathway. The results demonstrate that DAla2GIP has protective properties on in H_2O_2-induced chondrocyte injury, this finding shows that novel GIP analogues have the potential as a novel therapeutic for OA patients.

Acknowledgments

This project was supported by the following: 1) National Natural Science Foundation of China, 81601949; 2) Fund Program for National International Scientific and Technological Cooperation, 2015DFA33050; 3) Fund Program for Basic Conditions Platform of Science and Technology in Shanxi Province, 201705D121010.

Funding

This study was supported by the National Natural Science Foundation of China (81601949), Fund Program for National International Scientific and Technological Cooperation (2015DFA33050) and Fund Program for Basic Conditions Platform of Science and Technology in Shanxi Province (201705D121010).

References

[1] A. Bortoluzzi, F. Furini, C.A. Scire, Osteoarthritis and its management - epidemiology, nutritional aspects and environmental factors, Autoimmun. Rev. (2018) (S1568-9972(18)30208-8 [pii]10.1016/j.autrev.2018.06.002).
[2] Q. Liu, X. Zhang, L. Dai, et al., Long noncoding RNA related to cartilage injury promotes chondrocyte extracellular matrix degradation in osteoarthritis, Arthritis Rheumatol 66 (4) (2014) 969–978, https://doi.org/10.1002/art.38309.
[3] J.Y. Kwon, S.H. Lee, H.S. Na, et al., Kartogenin inhibits pain behavior, chondrocyte inflammation, and attenuates osteoarthritis progression in mice through induction of IL-10, Sci. Rep. 8 (1) (2018) 13832, https://doi.org/10.1038/s41598-018-32206-710 (1038/s41598-018-32206-7 [pii].).
[4] N. Fahy, M. Alini, M.J. Stoddart, Mechanical stimulation of mesenchymal stem cells: implications for cartilage tissue engineering, J. Orthop. Res. 36 (1) (2018) 52–63, https://doi.org/10.1002/jor.23670.
[5] Y. Wang, X. Sun, J. Lv, et al., Stromal cell-derived factor-1 accelerates cartilage defect repairing by recruiting bone marrow mesenchymal stem cells and promoting chondrogenic differentiation < sup/ > , Tissue Eng Part A 23 (19–20) (2017) 1160–1168, https://doi.org/10.1089/ten.TEA.2017.0046.
[6] Y. Seino, D. Yabe, Glucose-dependent insulinotropic polypeptide and glucagon-like peptide-1: incretin actions beyond the pancreas, J Diabetes Investig 4 (2) (2013) 108–130, https://doi.org/10.1111/jdi.12065JDI12065 (pii).
[7] W. Ramsey, C.M. Isales, Intestinal incretins and the regulation of bone physiology, Adv. Exp. Med. Biol. 1033 (2017) 13–33, https://doi.org/10.1007/978-3-319-66653-2_2.
[8] S. Shimazu-Kuwahara, Y. Kanemaru, N. Harada, et al., Glucose-dependent insulinotropic polypeptide deficiency reduced fat accumulation and insulin resistance, but deteriorated bone loss in ovariectomized mice, J Diabetes Investig (2018), https://doi.org/10.1111/jdi.12978.
[9] K. Fulzele, T.L. Clemens, Novel functions for insulin in bone, Bone 50 (2) (2012) 452–456, https://doi.org/10.1016/j.bone.2011.06.018S8756-3282(11)01059-3 (pii).
[10] A. Mieczkowska, B. Bouvard, D. Chappard, et al., Glucose-dependent insulinotropic polypeptide (GIP) directly affects collagen fibril diameter and collagen cross-linking in osteoblast cultures, Bone 74 (2015) 29–36, https://doi.org/10.1016/j.bone.2015.01.003S8756-3282(15)00007-1 (pii).
[11] Q. Zhong, K.H. Ding, A.L. Mulloy, et al., Glucose-dependent insulinotropic peptide stimulates proliferation and TGF-beta release from MG-63 cells, Peptides 24 (4) (2003) 611–616 (DOI: S0196978103001037 [pii]).
[12] K.H. Ding, X.M. Shi, Q. Zhong, et al., Impact of glucose-dependent insulinotropic peptide on age-induced bone loss, J. Bone Miner. Res. 23 (4) (2008) 536–543, https://doi.org/10.1359/jbmr.071202.
[13] G. Mabilleau, B. Gobron, A. Mieczkowska, et al., Efficacy of targeting bone-specific GIP receptor in ovariectomy-induced bone loss, J. Endocrinol. (2018), https://doi.org/10.1530/JOE-18-0214 DOI: JOE-18-0214 [pii].
[14] Y. Wang, L. Wei, L. Zeng, et al., Nutrition and degeneration of articular cartilage, Knee Surg. Sports Traumatol. Arthrosc. 21 (8) (2013) 1751–1762, https://doi.org/10.1007/s00167-012-1977-7.
[15] Y. Ding, L. Wang, Q. Zhao, et al., MicroRNA93 inhibits chondrocyte apoptosis and inflammation in osteoarthritis by targeting the TLR4/NFkappaB signaling pathway, Int. J. Mol. Med. 43 (2) (2019) 779–790, https://doi.org/10.3892/ijmm.2018.4033.
[16] H.S. Hwang, H.A. Kim, Chondrocyte apoptosis in the pathogenesis of osteoarthritis, Int. J. Mol. Sci. 16 (11) (2015) 26035–26054, https://doi.org/10.3390/ijms161125943ijms161125943 (pii).
[17] J.L. Berlier, I. Kharroubi, J. Zhang, et al., Glucose-dependent insulinotropic peptide prevents serum deprivation-induced apoptosis in human bone marrow-derived mesenchymal stem cells and osteoblastic cells, Stem Cell Rev. 11 (6) (2015) 841–851, https://doi.org/10.1007/s12015-015-9616- 610.1007/s12015-015-9616-6 (pii).
[18] G. Mabilleau, R. Perrot, A. Mieczkowska, et al., Glucose-dependent insulinotropic polypeptide (GIP) dose- dependently reduces osteoclast differentiation and resorption, Bone 91 (2016) 102–112, https://doi.org/10.1016/j.bone.2016.07.014S8756-3282(16)30194-6 (pii).
[19] A. Mieczkowska, N. Irwin, P.R. Flatt, et al., Glucose-dependent insulinotropic polypeptide (GIP) receptor deletion leads to reduced bone strength and quality, Bone 56 (2) (2013) 337–342, https://doi.org/10.1016/j.bone.2013.07.003S8756-3282(13)00252-4 (pii).
[20] E. Maneiro, M.A. Martin, M.C. de Andres, et al., Mitochondrial respiratory activity is altered in osteoarthritic human articular chondrocytes, Arthritis Rheum. 48 (3) (2003) 700–708, https://doi.org/10.1002/art.10837.
[21] A. Kocyigit, E.M. Guler, Curcumin induce DNA damage and apoptosis through generation of reactive oxygen species and reducing mitochondrial membrane potential in melanoma cancer cells, Cell Mol Biol (Noisy-le-grand) 63 (11) (2017) 97–105, https://doi.org/10.14715/cmb/2017.63.11.17.
[22] G. Musumeci, P. Castrogiovanni, F.M. Trovato, et al., Biomarkers of chondrocyte apoptosis and autophagy in osteoarthritis, Int. J. Mol. Sci. 16 (9) (2015) 20560–20575, https://doi.org/10.3390/ijms160920560ijms160920560 [pii].
[23] C. Liu, Y. Ye, Q. Zhou, et al., Crosstalk between Ca2+ signaling and mitochondrial H2O2 is required for rotenone inhibition of mTOR signaling pathway leading to neuronal apoptosis, Oncotarget 7 (7) (2016) 7534–7549, https://doi.org/10.18632/oncotarget.71837183 (pii).
[24] F.D. Toledo, L.M. Perez, C.L. Basiglio, et al., The Ca(2)(+)-calmodulin-Ca(2)(+)/calmodulin-dependent protein kinase II signaling pathway is involved in oxidative stress-induced mitochondrial permeability transition and apoptosis in isolated rat hepatocytes, Arch. Toxicol. 88 (9) (2014) 1695–1709, https://doi.org/10.1007/s00204-014-1219-5.
[25] B.T. McDermott, S. Ellis, G. Bou-Gharios, et al., RNA binding proteins regulate anabolic and catabolic gene expression in chondrocytes, Osteoarthr. Cartil. 24 (7) (2016) 1263–1273, https://doi.org/10.1016/j.joca.2016.01.988.
[26] C.B. Little, A. Barai, D. Burkhardt, et al., Matrix metalloproteinase 13-deficient mice are resistant to osteoarthritic cartilage erosion but not chondrocyte hypertrophy or osteophyte development, Arthritis Rheum. 60 (12) (2009) 3723–3733, https://doi.org/10.1002/art.25002.
[27] J. Shen, Y. Abu-Amer, R.J. O'Keefe, et al., Inflammation and epigenetic regulation in osteoarthritis, Connect. Tissue Res. 58 (1) (2017) 1–21, https://doi.org/10.1080/03008207.2016.1208655.
[28] V. Balaganur, N.N. Pathak, M.C. Lingaraju, et al., Chondroprotective and anti-inflammatory effects of S- methylisothiourea, an inducible nitric oxide synthase inhibitor in cartilage and synovial explants model of osteoarthritis, J. Pharm. Pharmacol. 66 (7) (2014) 1021–1031, https://doi.org/10.1111/jphp.12228.
[29] C. Lu, Y. Li, S. Hu, et al., Scoparone prevents IL-1beta-induced inflammatory response in human osteoarthritis chondrocytes through the PI3K/Akt/NF-kappaB pathway, Biomed. Pharmacother. 106 (2018) 1169–1174 DOI: S0753-3322(18)32773-2 [pii] https://doi.org/10.1016/j.biopha.2018.07.062.
[30] S.F. Ahmad, M.A. Ansari, K.M. Zoheir, et al., Regulation of TNF-alpha and NF-kappaB activation through the JAK/STAT signaling pathway downstream of histamine 4 receptor in a rat model of LPS-induced joint inflammation, Immunobiology 220 (7) (2015) 889–898, https://doi.org/10.1016/j.imbio.2015.01.008S0171-2985(15)00010-8 (pii).
[31] M.H. Park, J.T. Hong, Roles of NF-kappaB in Cancer and inflammatory diseases and their therapeutic approaches, Cells 5 (2) (2016), https://doi.org/10.3390/cells5020015E15 ([pii]cells5020015 [pii].).